Conditions for blister formation during thermal cycles of Al–Si–Cu–Fe alloys for high pressure die-casting

Oksana Ozhoga-Maslovskaja, Elisabetta Gariboldi *, Jannis Nicolas Lemke

Politecnico di Milano, Department of Mechanical Engineering, Via La Masa 1, 20156 Milan, Italy

The mechanism of blister formation during thermal cycle in a High Pressure Die Cast Al–9Si–3Cu–Fe alloy (EN 46000) was investigated by means of FEM simulation of a pressurized subsurface defect, considering the high-temperature elastoplastic behavior experimentally derived. The effect of parameters related to initial defect geometry, location and maximum temperature was analyzed. Blister formation was considered to occur as the maximum surface displacement after a thermal cycle exceeded 0.005 mm. It was shown that, for a given reference gas pressure, pore volume and depth, as well as temperature, blisters were developed from pores below a critical aspect ratio, as a result of high plastic strain accumulation in localized regions laying between the pore and the outer surface (ligament). Similarly, critical ligament thickness was identified and correlated to temper-ature and reference gas pressure. The development of blisters at temperatures lower than 400 °C from pores with reference pressure 90 MPa was predicted for a wide range of aspect ratios and ligament thickness. The possible occurrence of blisters in conventional HPDC components during heat treatment cycles at 350 °C was modeled for different pore pressures in the case of surface-near defects, mainly from lamina-shaped pores and was experimentally confirmed.

Keywords:
Blister
High pressure die casting
Thermal cycle
Al–9Si–3Cu–Fe alloy (EN 46000)
High temperature behavior

1. Introduction

The possibility to improve the mechanical properties of high pressure die-cast (HPDC) components made of age-hardenable Al–Si based alloys by means of suitable heat treatments, typically solution treatment followed by artificial aging, attracted the attention of designers and foundries in recent years. The effects of material composition and thermal cycle on mechanical properties of cast parts have been modeled in order to design optimal heat treatment cycles, as it is shown in the work of Sjolander [1]. Further, heat treatment cycle on these components can also be of different type, sometimes performed to meet other industrial needs. However, the potentialities offered by heat treatments must cope with increased process costs and with the risk of giving rise to defects. These could be either of geometrical type, such as distortions caused by local strains of thermal origin or of surficial type, such as blistering, as illustrated experimentally by Lumley et al. [2].

From a morphological point of view, blisters consist in small amounts of material that blow up with respect to the surrounding surface. On a smooth die cast part, a local change of the surface position of about a few hundredths of millimeters is sufficient to consider the part unusable by esthetical or functional reasons.

* Corresponding author.
E-mail addresses: oksana.ozhogamaslovsk@polimi.it (O. Ozhoga-Maslovskaja), elisabetta.gariboldi@polimi.it (E. Gariboldi), jannisnicolas.lemke@polimi.it (J.N. Lemke).

In general, the formation of blisters during thermal cycles of cast part following its extraction from the die, can take place whenever a gas-containing subsurface discontinuity lays close to the outer surface and temperature is high. As a matter of fact, at elevated temperature the pressure becomes so high within these discontinuities to plastically deform the covering surface layer, which yield stress is relatively low at high temperature [3]. The phenomenon is typical in HPDC metallic part where the metal flow is of turbulent type. Due to the increased air entrapment the inner pressure inside these discontinuities at solidi-fication temperature is high.

Even if blisters can form during ejection from the die when cast parts are still at a high temperature, their occurrence is more critical during following heat treating steps, specifically those performed at high temperature, such as solution treatments. The blister formation is well illustrated for alloy 360 in the work of Lumley et al. [2], where authors observed surface blistering and discoloration after 16 h at 545 °C. Niu et al. [4] presented micrographs of Al–18%Si alloy after T6 tempering with distorted surface morphology due to the gas (mainly air) expansion.

The blister formation described above should not be confused with outgassing, sometimes also referred to as blistering, where a coating layer blows up due to gas inclusions flowing out from the metal, as a result of deformation up to rupture of the thin surface metallic layer [3]. This latter case of blistering is related only to coated cast parts and will not be taken into account in the present study.

Published Journal Article available at: http://dx.doi.org/10.1016/j.matdes.2015.12.003

At least three groups of factors and their dependence on temperature act concurrently on blister formation:

- the pressure of the gas(mainly air, but also gas developing from die spray or other organic materials)inside the pore;
- the initial geometrical discontinuity features such as shape and location;
- the mechanical properties of the alloy in the temperature range of interest.

The gas pressure inside the pore in the solidified metal is significant-ly affected by temperature and is typically estimated in models by means of the simple gas law once the pressure at a reference tempera-ture is known. One possibility is to consider the reference pressure level close to the solidus temperature of the alloy of interest. The evaluation of the actual gas pressure (p_a) inside pores of cast parts at this temper-ature is not an easy task. On one side p_a is related to fluid dynamics of die filling and varies highly from one region to another of the same cast part. Neglecting the effect of the die geometry and the presence of other gases such as those dissolved into the liquid, such as hydrogen, the pressure of gas entrapped in the liquid can be only related to the vol-ume and initial pressure of the air inside the die cavity. The initial pres-sure is affected by the efficiency of the air evacuation system, filling time and the pressure acting on the liquid. Simple models such as the one presented by Homayonifar et al. [5] allow estimation of the effect of the casting features, which have been key points for several innovative HPDC technologies for recent years, that the reader can find in the re-view works of Thirugnahan [6] and Uchida [7] among others.

After the filling is completed, during solidification of the alloy, a further movement of the plunger in the so called intensification stage causes an applied pressure (p_{ext}) to act on the liquid metal in addition to the metallostatic one [8]. This latter is negligible with respect to the first one, which in conventional HPDC processes ranges from 20 up to about 100 MPa, 5–40% less than the set intensification pressure, as it was experimentally demonstrated in the work of Dargusch et al. [9]. The applied pressure (p_{ext}) prevents the presence of spherical pores of radius lower than a critical value (r_c) in the liquid phase, correlated not only to the pressure of the entrapped gas (p_a), but also to the pres-ence of the gas–liquid interface tension (γ) and to the metallostatic pressure (p_H) [8]. Neglecting this latter term, the critical radius can be calculated as following:

$$r_c = \frac{2\gamma}{p_a - p_{ext}} = \frac{2\gamma}{\Delta p}. \quad (1)$$

Due to the fast cooling during HPDC processes, the growth rate of the pore size in liquid can be assumed to be zero. Further, the effect on the pressure of entrapped gas(p_a)due to solidification shrinkage can be neglected. As a result r_c can be assumed as the minimum pore size. The Δp leading to critical radii of the range of 10 μm is about 0.2 MPa for the surface energy values of non-oxidized or oxidized Al (1.1 and 0.816 N/m, respectively [9]) which are in a similar range of the investi-gated alloy. This amount is negligible compared to the applied pressure during the intensification stage (p_{ext}). Thus, particularly in the case of larger voids, the probability to form blister is far less, because the pres-sure of the entrapped air is comparable to the applied one.

Regarding the geometrical features which can affect blister formation, the main ones are the defect shape and depth of the sub-surface defect, affecting the thickness and thus the stiffness and strength of the ligament. The gas-entrapment porosity is often referred and modeled as being spherical, with smooth surfaces [3,9]. However, due to pressure effect these spheres can be reduced to ellipsoids and air-entrapment voids can combine to shrinkage porosity, originating a rougher pore on which dendrites can appear [4,10]. Gas-porosity could also lead to laminations [3], which can include small pores elongated or clustered along a subsurface layer filled with air and/or organic materials potentially transforming into pressurize gases.

Finally, the alloy composition and initial microstructural conditions influence the development of blisters on the cast part surface. During die-filling and solidification the alloy composition affects the thermophysical properties of the metal, which can be correlated to the average size and inner pressure of the pores, as shown experimentally by Niu et al. [4] for Al–Si alloys containing 5, 8 and 18% Si.

The aim of the present paper is to offer a tool for evaluating the effects of heat cycle temperature and of subsurface pore features (such as internal pressure and geometry) on the possibility to develop blister from it. The effects of alloy composition are not addressed, focusing the attention on a widely applied Al–Si based alloy. The method could be potentially extended to other alloying systems and production processes causing air- or gas-containing sub-surface discontinuities.

2. Problem statement

The external surface of an Al–Si–Cu-based HPDC alloy part is shown in Fig. 1a. The microstructure is made of homogeneously distributed α phase and eutectic grains.

Depending on the local different solidification conditions in a cast part, a surface 'skin' layer characterized by a finer structure of outer eutectic-rich and inner alpha-rich zones of various thickness and morphology can form. Below the surface skin appears the bulk microstructure with different microstructural features and material properties. Blisters form due to the presence of sub-surface discontinuities of certain size, shape and position. In principle they can lay both in the skin layer and in the bulk material and typically they are situated far enough from each other to consider them as single defects. Furthermore, the size of the voids potentially evolving into blister during heat treatment allows modeling of the microstructure by considering the homogeneous material both in the bulk and in the skin layers.

The portion of the material originating blisters is described by means of the simplified geometrical model shown in Fig. 1b consisting of a solid parallelepiped with an external skin layer, a bulk portion and a single pore. The lateral size and the height of this portion should be taken sufficiently large so that the external parts of the portion corresponding to the bulk material are not affected by the presence of the pore. The pore is assumed to have an elliptical shape with the main axes A and C. The pore position is described by a distance D, corresponding to the depth of the center of the pore. The pore is filled with air, at pressure p_0 at room temperature (25 °C).

The ranges of the geometrical features and of air pressure are discussed in the following section related to the finite element modeling. As a first approach, the presence of the skin layer is neglected, thus considering the material properties as homogeneous.

3. Material model description

The problem is solved for one of the most commonly used die-casting alloys: EN 46000 alloy, also referred as EN AC AlSi9Cu3Fe, thus characterized by the nominal presence of 9 mass% of Si and 3 mass%of Cu. Due to the homogeneity and continuity assumptions, the mechanical properties of the fully dense alloy at temperatures of interest are considered. The material is assumed to behave elastic-plastically, neglecting possible creep effects at elevated temperatures. The elastic part is described by a constant Poisson's ratio of 0.3 and a longitudinal elastic modulus E depending on temperature, which was extracted from quadratically fitting literature data [11]. The E value at RT is 69 GPa, at 300 °C is 53 GPa and at 450 °C is 40 GPa. Stress–strain curves were obtained from laboratory tension tests carried out in the range of 25–450 °C on a set of suitable die-cast specimens, the publication on the experimental procedure and obtained results is planned. The specimens were produced by combining and optimizing a die and manufacturing

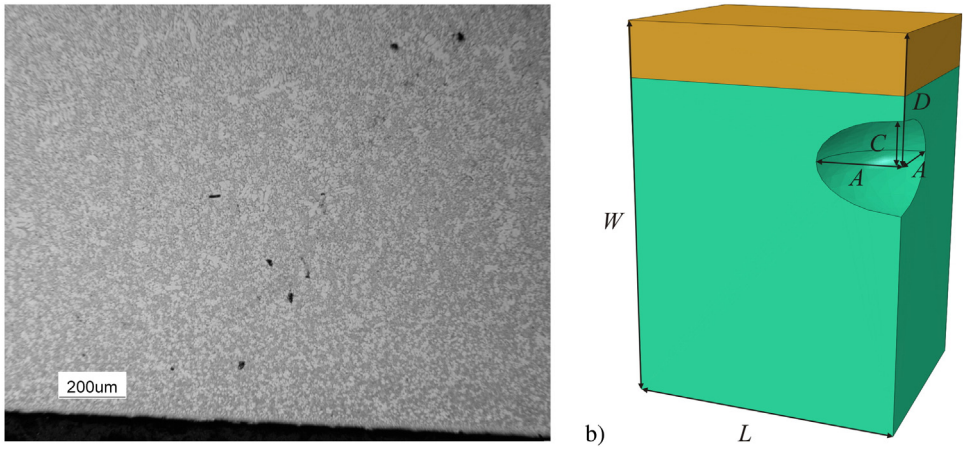

Fig. 1. a) Representative microstructure of an Al alloy high pressure die cast part; b) geometrical description of the material portion containing a defect filled with air.

system that allowed a very low level of porosity and a controlled microstructure as it is described by Timelli et al. [12,13]. The true stress vs. true plastic strain correlation is described, employing the power law relationship [14]:

$$\sigma = K_T \cdot \varepsilon^{n_T}, \tag{2}$$

where K_T and n_T are temperature dependent material parameters, having the meaning of the strain hardening coefficient and strain hardening exponent. Experimentally obtained temperature dependence (temperature T in °C) of the material parameters K_T and n_T was obtained by data fitting using the following polynomial cubic relationship:

$$f(x) = A_0 + A_1 \cdot T + A_2 \cdot T^2 + A_3 \cdot T. \tag{3}$$

Table 1 lists the polynomial multipliers describing the temperature dependence of the parameters K_T and n_T, presented in graphical form in Fig. 2.

4. FE model description

The model was developed to investigate the local stress state in the vicinity of the separated subsurface defect, assumed to have an axisymmetric shape, subjected to axisymmetric loading conditions. The 2D axi-symmetric mechanical problem of the pore is presented in Fig. 3. The symmetry axis *Y* of the model coincides with the pore axis normally oriented to the surface. The boundary conditions are given in the same figure, where vertical displacement is set to zero at the bottom edge of the model (where $X = 0$). The air/metal interface identifying the pore is subjected to a normally applied uniform pressure p. All other edges are left free, according to the basic assumption that constraints/stresses related to thermal cycle or to the presence of other discontinuities could be neglected.

In order to investigate the influence of the pore depth and geometry, as well as that of the value of applied pressure and temperature on the stress strain state in the model material, a Python code allowing the automatic building of the geometric features and a finite element model in Abaqus software is created. The geometrical and loading parameters as well as the element size are given in a parametric form, which allows the user to carry out easily sets of calculations. As an example, lateral size of the portion (L) is fixed at three times of the radius parallel to the surface (A), while the width (W) is set to be 6 times of the radius perpendicular to the surface (C). The element size is controlled by the ratio $L/20$ and an additional mesh refinement close to the pore edge is done to produce accurate evaluation of the stresses acting there. Pore geometry is defined by means of the C/A ratio, ranging from 0.06 to 2. The first case represents the case of laminae and the second one the pores slightly elongated toward the surface. The size of the pores is de-fined on the basis of the radius A. Relatively low values of A have been taken into account for the present simulations (0.0015–0.015 mm), where the main focus is on the effect of the pore shape and depth, but the possibility to scale up the obtained result for larger pores will be illustrated later. Furthermore, the axial position of pore is identified by means of the geometrical parameter H, defined as $H = D - C$, corre-sponding to the external ligament thickness. It has been varied in order to check the case of extremely thin or thick ligament compared to the pore size (respectively, 0.0004–0.152 mm).

Fully coupled thermal-stress analysis is chosen, in order to enable the simultaneous calculation of displacements, depending both on tem-perature and mechanical loading conditions. The reduced-integration quadratic elements for the coupled temperature-displacement analysis are used.

The tabular values of the simulated stress–strain curve at given temperature are obtained from the elaboration of experimental high-tem-perature tensile tests described in the previous section. When the tabular range of strains is exceeded, the isotropic hardening behavior is taken into account. Other material parameters, required by the soft-ware for the temperature analysis of the investigated alloy are taken from literature [11] and are listed in Table 2.

Parameters in Table 2 are assumed to be constant with temperature, although in the reality it is not the case, except of thermal conductivity. Experimental data in [15] showed, that in temperature range from 0 to 500 °C thermal conductivity of aluminum is almost constant with the temperature. Preliminary simulations on the current model showed that the amount of strains caused by temperature change is significantly lower in comparison to plastic strains generated by internal pressure. Thus, the inaccuracy caused by the assumption is negligible small.

Since FE simulations are carried out to investigate the development of blisters during thermal cycles, a generic triangular one is reproduced. The lower temperature T_0 corresponds to room temperature and the upper temperature T_h to the heat treatment temperature. The simula-tion includes the cooling step in order to obtain the surface morphology at the end of the whole thermal cycle. Creep behavior is not taken into account in the description of the mechanical behavior of the alloy and, as a result, the length of time intervals, defining the thermal cycle is

Table 1
Values of polynomial multipliers used in the description of the Al alloy EN 46000 temperature-dependence of the parameters K_T and n_T as in Eqs. (2) and (3).

	A_0	A_1	A_2	A_3
$K_T(x)$, [MPa]	613	-0.59	$-4.9 \cdot 10^{-3}$	$7.3 \cdot 10^{-6}$
$n_T(x)$, [mm/mm]	0.21	$-1.3 \cdot 10^{-4}$	$-1.1 \cdot 10^{-6}$	$1.1 \cdot 10^{-9}$

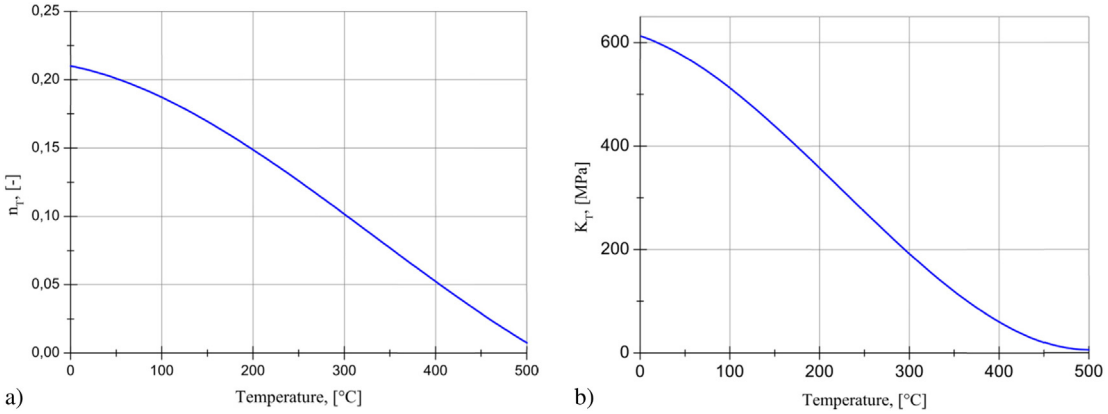

Fig. 2. Temperature dependence of material parameters: a) n_T; b) K_T, derived from experimental data for the Al alloy EN 46000.

not relevant. Each period is defined to have a unit length and is rather related to the analysis time.

Concerning the loading history connected to the thermal one, the pressure change is assumed to be only correlated to temperature, not to the change of volume of the pore occurring at high temperature. Thus, the following relation is used for pressure evaluation:

$$\frac{p_0}{T_{0+273}} = \frac{p_h}{T_{h+273}} = \frac{p_s}{T_{s+273}}, \tag{3}$$

where p_0, p_h and p_s refer to the pressure at room temperature, heat treatment temperature and solidus temperature, respectively. For the nominal composition of the investigated alloy T_S is 528 °C [12]. In the in-vestigated temperature range the conservation of pore volume assump-tion leads to an overestimation of the pressure value of about 1.2%,

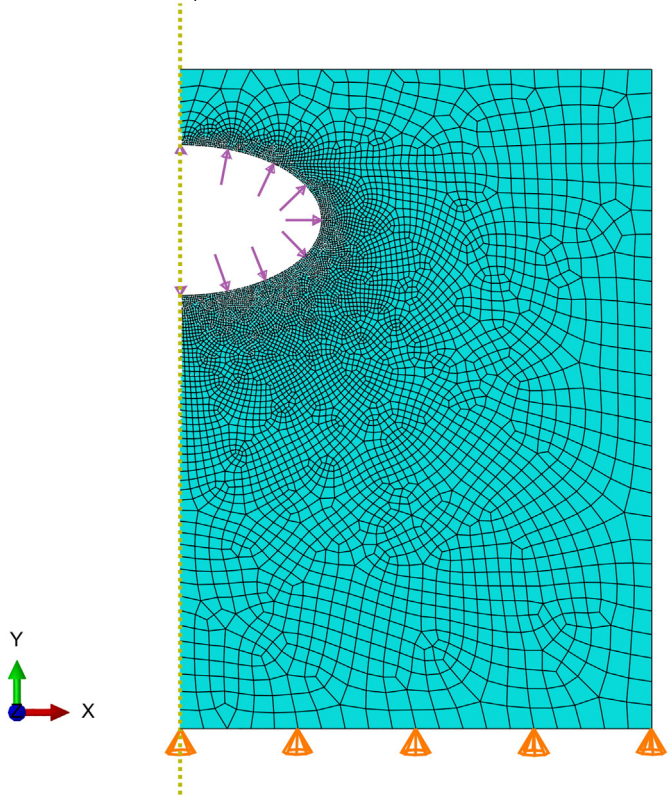

Fig. 3. Axisymmetric FE model of the solid, containing an elliptic pore with applied boundary conditions and inner pore pressure.

which could be neglected without reducing the accuracy of the simulation significantly.

As mentioned in the introduction, the estimation of the actual inner pore pressure at solidification temperature (p_s) is complex, even if it is strongly affected by the pressure applied to the liquid when solidifica-tion takes place. In the current simulation three reference levels of p_s are taken into account: 30, 60 and 90 MPa. In this way the wide range of conditions during HPDC parts production is covered.

5. FEM predictions

5.1. Local analysis of pore deformation

The plastic strains distribution at different temperature steps of the thermal cycle in the vicinity of the pore is displayed in Figs. 4 and 5 on the corresponding deformed shape of the FE model. In two considered situations the reference pressure p_s is set to 30 MPa, but the inner pores are characterized by different shape and size.

The pore shown in Fig. 4 is characterized by a relatively rounded shape, slightly elongated below the surface, having a *C/A* value of 0.53 that is considered as a reference for this model. The pore volume equals $7.5°10^{-6}$ mm^3, considered as a second reference condition and corre-sponds for this specific case to $A = 0.015$ mm. The location of this pore is defined by a ligament thickness *H* equal to 0.0245 mm and de-fines a relatively deep-seated defect. Fig. 4 shows the strain field dia-grams at the selected steps of a heat treatment cycle with $T_h =$ 440 °C. The results are presented only on the part of model, significant for the results interpretation. As the temperature reaches 380 °C, localized plastic deformations accumulate in the material surrounding the pore at a radius *A*. With the temperature increase the material expands and moves toward the surface as well as the corresponding maximum principal plastic strains field. A maximum limit for the displayed strains is set to 0.2 mm/mm for all the images, the greater values are represented by the same color as the maximum limit value. Thus, even if the material model description does not include any damage nor fracture criteria, zones with the maximum limit strain value suggest regions where the material would reasonably be extensively damaged or frac-tured. For the simulated pore these regions can be seen at the heat treat-ment temperature of 440 °C, while at 420 °C the maximum principal strain is of the order of 0.1 mm/mm. In a temperature range of 20 °C

Table 2
Selected properties of investigated alloy.

Density, [kg/dm^3]	2.74
Specific heat at 100 °C, [J/(g·K)]	0.88
Coefficient of thermal expansion, [1/K]	$2.1·10^{-5}$
Thermal conductivity, [W/(m·K)]	110

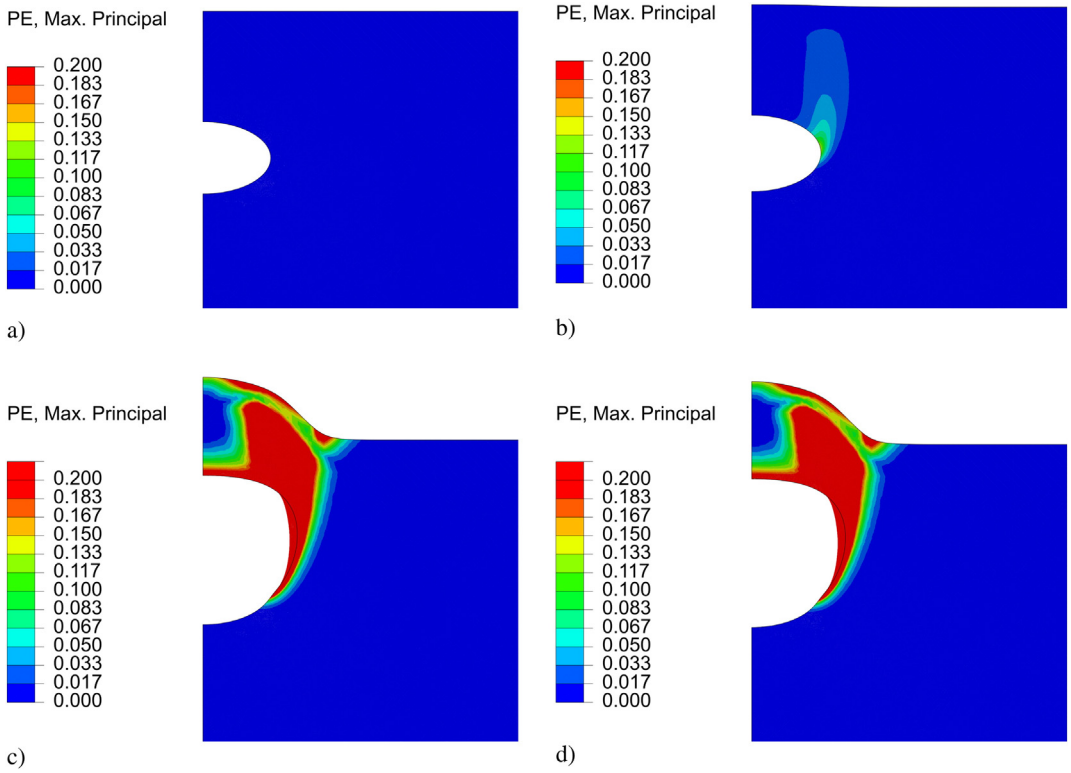

Fig. 4. Localized plastic strains generated by the pore with $C/A = 0.53$, $7.5°10^{-6}$ mm^3 pore volume, $H = 0.0245$ mm and reference inner pressure p_s of 30 MPa at different temperatures during heating: a) 25 °C; b) 420 °C; c) 440 °C and d) at room temperature $T_0 = 25$ °C after cooling. Note that the color scale for plastic strains, plotted on the deformed shape limited by the value of maximum principal plastic strains equal to 0.2 mm/mm.

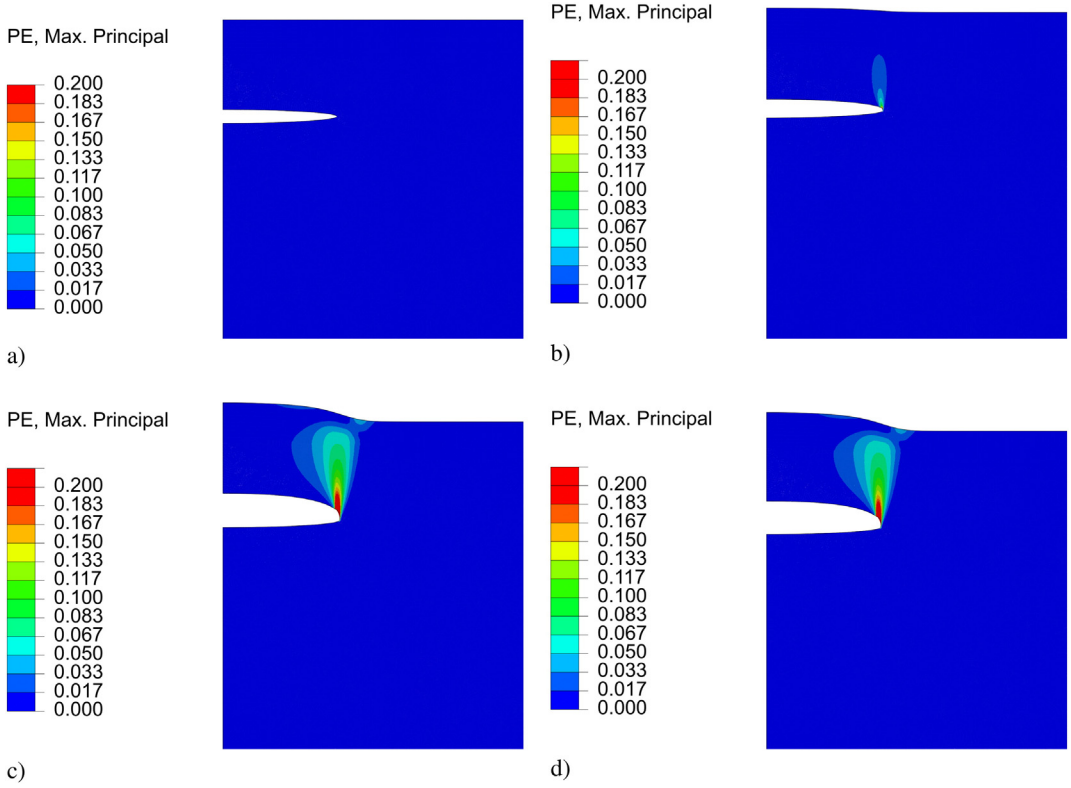

Fig. 5. Localized plastic strains generated by the pore with $C/A = 0.06$, pore volume of $7.5°10^{-6}$ mm^3, $H = 0.0245$ mm and reference inner pressure p_s of 30 MPa at different temperatures during heating: a) 25 °C; b) 360 °C; c) 390 °C; d) and at room temperature ($T_0 = 25$ °C) after cooling. Also in these figures the plastic strains are plotted on the deformed shape and the notes about the color scales for Fig. 4 are to be considered. (For interpretation of the references to color in this figure legend, the reader is referred to the web version of this article.)

one can see rapid plastic strain increase up to the maximum limit value. The corresponding behavior of the vertical displacement of the free surface just above the pore (Y_{surf}) can be considered as the height of the formed blister. In any case, the extremely high localized plastic strain values can be treated as the appearance of a blister or as its 'opening' under the applied inner pore pressure. Fig. 4 also shows that the ellipsoidal pore initially slightly flattened below the surface (with $C/A = 0.53$) significantly deforms at high temperature and gets closer to the surface.

The evolution of the plastic strain field on the deformed shape occurring during heat treatment cycle within the investigated FE model in the case of the second pore shape, characterized by lower C/A ratio, the same pore volume and the same ligament thickness, is shown in Fig. 5. The heat treatment temperature in this case has been limited to 390 °C, above which the extremely high plastic strain values does not corresponded to realistic blistering or opening conditions. The compar-ison between the effects of temperature on the two pores of the same volume and reference inner pressure (p_s) clearly shows that the onset of blisters is heavily affected by the defect shape, being more critical for laminar discontinuities, with low C/A ratios.

5.2. Dependence on pore shape

Several simulations of the model behavior during a thermal cycle have been performed obtaining results similar to those displayed in Figs. 4 and 5. The obtained results are given in the following paragraphs in order to analyze the different geometrical, loading and thermal parameters on the formation of blisters. The resulting condition at the end of a thermal cycle has been summarized by means of the axial displacement of the free surface just above the pore $Y_{surf.}$

In the first set of simulations, the effect of pore shape and depth, described in terms of C/A and H parameters is evaluated. The value of pore volume is kept constant and set to $7.5°10^{-6}$ mm^3 (as for the cases shown in Figs. 4 and 5). Simulations are carried out at pressure p_s of 30 MPa and a temperature of 370 °C, at which the preliminary ma-terial behavior simulations and previous experimental observations show that blister formation can occur.

The minimum aspect ratio corresponds to an oblate ellipsoid, parallel to the surface, which approaches disc-shaped discontinuities and models the presence of defects such as laminar distributed porosity. The local stress–strain field developed by defects with small C/A ratio can also correspond to conditions of combined effect of shrinkage and the presence of gas/air porosity. Three values of H are considered for this set of simulations: 0.014, 0.010 and 0.004 mm.

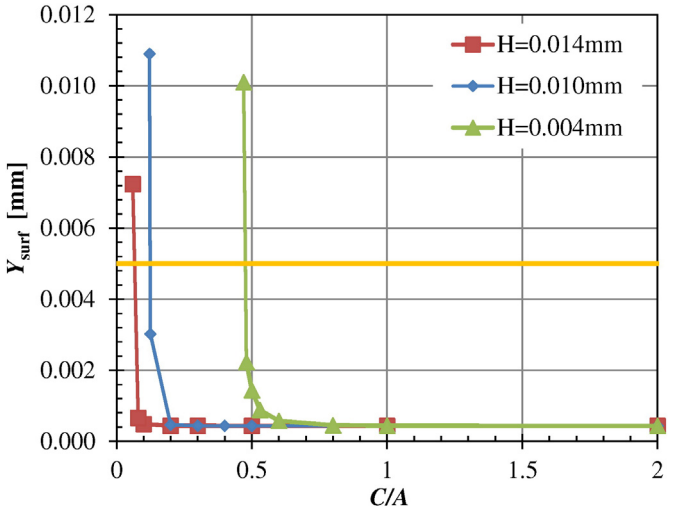

Fig. 6. Dependence of surface maximum displacement (Y_{surf}) on the pore aspect ratio C/A for a constant pore volume of $7.5°10^{-6}$ mm^3, $p_s = 30$ MPa and $T_h = 370$ °C.

The results of simulation are summarized in Fig. 6, where the magnitude of the maximum axial displacement at the end of a thermal cycle is related to aspect ratios for the three H levels. The plot clearly shows that the external ligament thickness plays an important role on blister formation, the smallest thickness being the most critical one. Furthermore, the plot shows that lower C/A (i.e. laminar shape of the pore) are more prone to blister formation. Such pores cause changes of surface morphology even at reasonably high values of external ligament thickness. Under the same pressure, temperature and ligament values, the spherical pore ($C/A = 1$) does not produce any detectable displacements at the free surface. This is the expected result as far as spherical shape is considered to be a perfect one to resister an internal pressure. The ligament thickness H significantly affects blister formation in the case of pores flattened below the surface (low C/A). For the lowest pore height value equal to 0.004 mm (which corresponds to the case of rather surficial defect) the spherical defect still does not generate displacements, while the pore with aspect ratio ($C/A = 0.53$) causes blistering.

The case of discontinuities characterized by higher C/A ratio is even less critical. The maximum aspect ratio corresponds to the oblate ellipsoid perpendicular to the surface. In this way positioned lamina does not generate any significant plastic strain field and does not pose a risk for blistering.

The value $C/A = 0.53$ is used in further analyses in order to predict the possibility of blister formation in cases of non-perfectly spherical pores. The presence of a blister at the end of the thermal cycle is assumed when the maximum surface height reaches the threshold value of 0.005 mm. The plot in Fig. 6 suggests that the maximum surface displacement is drastically affected by small C/A modifications. Thus, the choice of the threshold value of maximum surface displacement only slightly affects the results of the simulation. The value of surface height corresponding to any given aspect ratio can be identified for each external layer thickness once a threshold axial surface displacement is considered.

5.3. Dependence on ligament thickness

In the previous analysis the critical role of the ligament thickness (H) on the blistering is shown. In order to extend this observation to the wider range of H (0.0049–0.0101 mm), the mechanical problem of the material portion containing a pore is solved for the case of reference

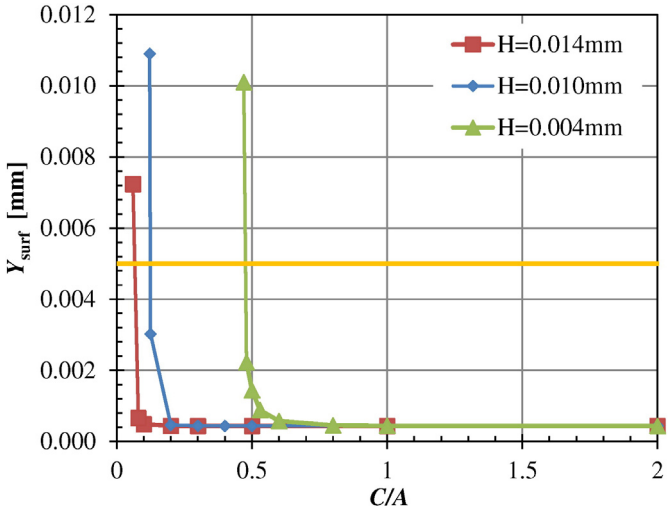

Fig. 7. Magnitude of the surface maximum displacement just above the pore (Y_{surf}), depending on the ligament thickness (H) for the reference pore geometry, pressure and temperature. Red vertical line corresponds to the critical ligament thickness (H_{cr}) below which blister forms at the investigated pore geometry, pressure and temperature. (For interpretation of the references to color in this figure legend, the reader is referred to the web version of this article.)

pore geometry ($C/A = 0.53$ and pore volume $7.5°10^{-6}$ mm^3), subjected to a reference pressure p_s of 30 MPa and held at $T_h = 370$ °C.

The results are represented in Fig. 7 in terms of Y_{surf}. For the pore and temperature conditions taken into account here, Y_{surf} values are rela-tively small for ligament thickness (H) greater than 0.006 mm, but they rapidly increase overcoming 0.005 mm as H decreases to a critical value (H_{cr}). The extremely fast increase of Y_{surf} for $H < H_{cr}$ suggests to consider H_{cr} as a threshold value for the forming or 'opening' of blisters below it.

To cover the wider range of technological conditions inherent to the investigated alloy, the mechanical problem is solved for the usual pore shape and size ($C/A = 0.53$ and pore volume $7.5°10^{-6}$ mm^3) at three reference pressure levels p_s: 30, 60 and 90 MPa and for temperatures T_h ranging from 300 to 490 °C. For each pressure and temperature a critical value of ligament thickness is evaluated as it is shown in Fig. 8. The correlation between the critical ligament thickness H_{cr} and heat treatment temperature T_h are plotted in Fig. 8 for each reference pres-sure level taken into account.

The curves represent the temperature T_h above which the pore evolves to a blister during the thermal cycle, considering the reference geometry, pressure p_s and a location at a depth corresponding to a liga-ment thickness H. When the combination of ligament thickness and temperature is represented by a point lying below the curve drawn for its reference pressure p_s, no blister will form, while points staying above the curve represent critical condition for the blister development. At the maximum reference pressure selected for these analyses ($p_s = 90$ MPa), the considered relatively small and rounded pore evolves into a blister at temperatures about 400 °C even if it is located at rela-tively high depth, with a ligament thickness approximately equal to its diameter. As the reference inner pressure decreases the safe range of combinations T_h and H extends. Further, at the lower investigated tem-peratures, the critical ligament thickness is less affected by temperature changes.

Due to the excessive extension of the plastic zone at elevated temperatures which depends on the reference pressure and ligament thickness, the curves are not given for temperatures higher than 490 °C, 440 °C and 400 °C for corresponding pressure levels of 30, 60 and 90 MPa. A different situation could also arise in the case of the pores located well under the surface (high H) as their inner pressure at these temperatures becomes very high, i.e. plastic deformations are mainly located around the pore, even for excessively high pressure values. Thus the pore does not evolve into a surface defect such as a blis-ter but could rather cause the extension of discontinuities from the pore surface, similarly to the microtomography observations done in work of Toda et al. [10] on HPDC pores held at high temperature.

5.4. Dependence on pore size

The influence of the pore size and heat treatment temperature on the value of critical ligament thickness H_{cr} is investigated. The represen-tative pore sizes are characterized by the minor axis C equal to 0.0008, 0.004 and 0.008 mm. The usual reference pore shape is characterized by the C/A ratio of 0.53 and reference pressure p_s of 30 MPa. The problem is solved for a set of T_h in the range of 360–490 °C.

The linear correlation between the critical ligament thickness H_{cr} and vertical pore size C at a fixed T_h can be observed in Fig. 9. This result can be compared with the analytical solution for the ideal case of thick-walled spherical shell, subjected to the inner pressure. In this case the collapse pressure due to yield for the case of elastic-perfectly plastic material behavior can be found linearly dependent on the ratio of the shell thickness to inner shell radius [16]. The investigated problem is much complex due to non-spherical pore geometry and the presence of the material below the pore, but nevertheless the ratio H/C can be considered as a scale factor in the simulated problem. The H_{cr}/C ratio could be used to scale H_{cr} at fixed T_h and p_s. However, each temperature displays a different H_{cr}/C ratio due to the different plastic strain field developed around the pore during heat treatment. The dependence of this ratio on T_h at p_s of 30 MPa, derived from data of Fig. 9,isillustrated in Fig. 10,where a 3rd order polynomial fitting line and its equation are also shown.

The H_{cr}/C ratio is strongly affected by heat treatment temperature due to easier development of plastic strains at high temperature where a more ductile material behavior is combined with higher inner pore pressures. Dividing the H_{cr} values at $p_s = 30$ MPa presented in Fig. 9 by C at each temperature level allows the evaluation of the temper-ature for blister development for pore of the same shape but different size. New different sets of curves could be obtained for different p_s and pore shapes. Figs. 9 and 10 can be used for the estimation of maximum heat treatment temperature in the case of pore of given shape, size and depth originated at a given p_s, or for the estimation of the minimum liga-ment thickness free from pores needed to avoid the formation of blisters at a given temperature T_h, with a well-defined pore volume and shape.

6. Discussion

The set of FE simulations of heat treatment cycle is performed on the representative surface portion of the investigated Al-alloy containing a pressurized ellipsoidal defect. The obtained results are far from supplying

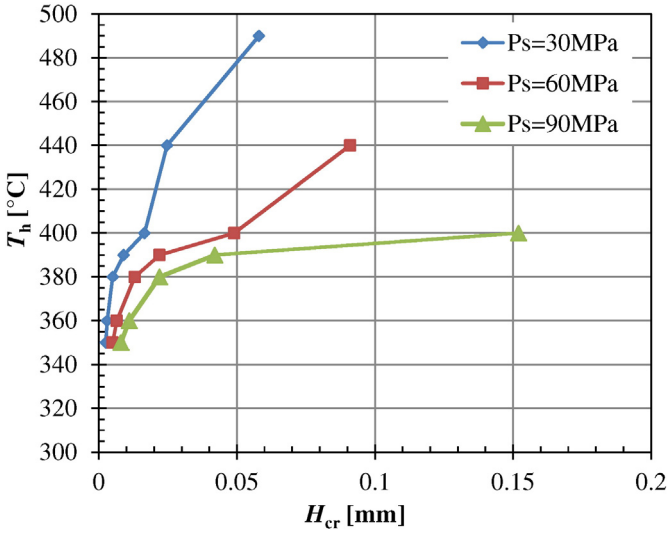

Fig. 8. Correlations between the critical ligament thickness H_{cr} and heat treatment temperature T_h for three considered reference pressure levels p_s.

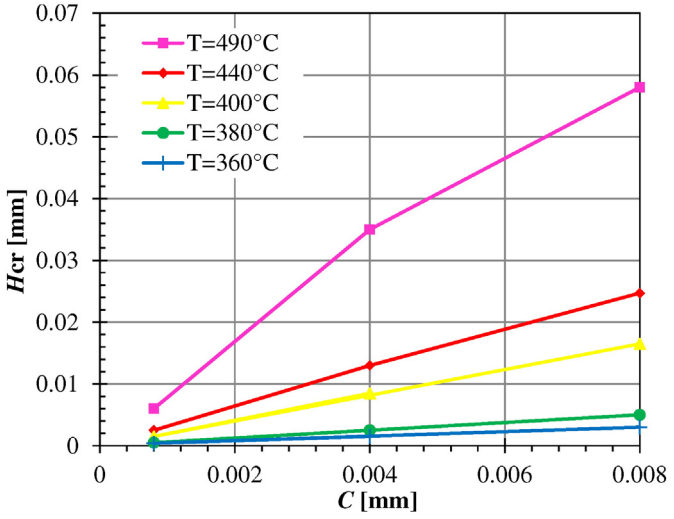

Fig. 9. Dependence of the H_{cr} on the pore radius C at different heat treatment temperatures (T_h) for the case of a pore with $C/A = 0.53$ and reference pressure $p_s = 30$ MPa.

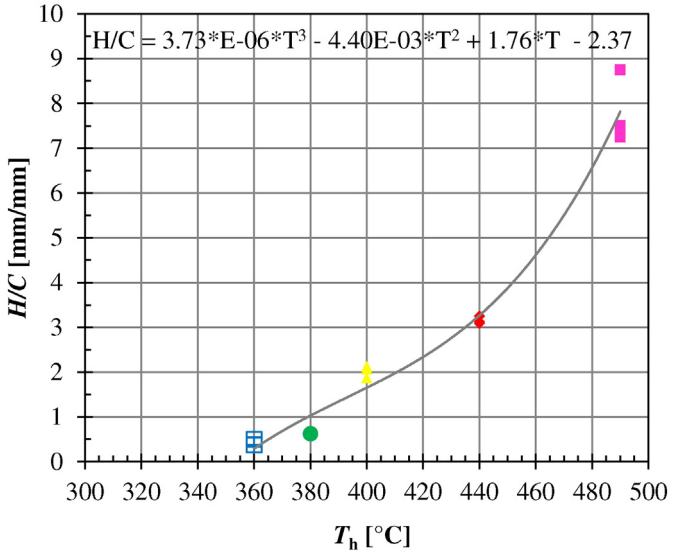

Fig. 10. Dependence of the ratio of the critical height H_{cr} to minor axis C on the heat treatment temperature) for the case of a pore with $C/A = 0.53$ and reference pressure $p_s = 30$ MPa.

the complete set of correlations between geometrical, thermal and loading parameters, but due to relatively wide covered range the prediction of their effect on blister formation during heat treatment can be given, as proposed in most of the examined cases, for pore shape characterized by aspect ratio $C/A = 0.53$. The appearance of blister is related to the development of plastic strains at high temperature in the material surrounding the pressurized pore. At a given temperature T_h and pressure, the plastic strain distribution is related to both C/A and H/C ratios, being con-sidered as shape and depth factors, respectively. As a result, also the ratio Y_{surf}/C will have the same trend as H_{cr}/C for pores, characterized by iden-tical C/A, p_s and T_h.

Despite the fact that for practical purposes Y_{surf} rather than Y_{surf}/C can be taken into account to identify the presence of blisters, also being unknown the pore size from which they developed, a rough estimation of critical temperatures, shape and pressure can be made by observing that Y_{surf} rapidly increases as H (and H/C with it) approaches critical value. Thus, the trends of both Y_{surf} and Y_{surf}/C will sug-gest the onset of blister.

A slightly different approach can be followed to check the effect of heat treatment temperature. Correlations, such as given in Fig. 10 allow derivation of temperature vs. H_{cr}/C correlation for each reference pressure level also accounting different initial pore size C. Thus, for the case of relatively low pressure, it represents a heat treatment temperature level above which pores with a given shape (C/A) develop blister for all relative depth (i.e. all H/C ratios). The evolution of plastic strains at different temperatures has shown that at high temperature and high inner pore pressure (related to both p_s and actual temperature) a critical condition is different from the problem considered here and rather corresponds to material damage arising from the subsurface pores, but in any case can be considered as critical for the component with pores of reference pressure p_s.

The plastic strain field and the corresponding deformed state of FE model shown in Fig. 4 are in perfect agreement with the morphology of the deformed subsurface rounded pore illustrated by the experimental works of Lumley [2], Niu [4] and Toda [10], mainly referring to the ef-fect of solution treatments. The progressive pore deformation toward the outer surface and a localized thinning of the ligament should be taken into account. Also the original size and location of the discontinu-ity should be identified from micrographs of heat treated parts consid-ering the inner part of the defect, less affected by geometrical changes. The proposed FE model predicted the formation of blisters from subsur-face discontinuities with the H/C ratio lower than 1 (with $p_s = 30$ MPa) even during heat treatments carried out at temperatures lower than 400 °C, i.e. well below the classical temperature range for solution treatments. This situation was experimentally observed in HPDC parts made of EN 46000 alloy heat treated at 350 °C. Metallographic sections containing blisters showed that the ligament thickness H was relatively thin compared to original C value (Fig. 11a). In the specific case of Fig. 11a, the pore shape suggests the coalescence of small pores into a single one, and the plastic strain localized in narrow regions within the ligament. Other metallographic sections of the same part confirmed no blister formation when pores were deeper, with higher H/C ratio exceeding 1.

Figs. 4 and 5, as well as the elaboration of other simulations clearly show the positive effects brought by the technological improvements aimed at reducing the reference inner pore pressure p_s at the end of the local solidification process. The results also suggest that, among pressurized discontinuities, the most critical are those flattened and lying parallel to the outer surface, referred here as laminas, from which blisters can arise easily even being located relatively deeply in-side the matrix and could additionally include gas developing from organic material during the same heat treatment. A laminar shape of discontinuity can also arise from the coalescence of several small voids formed at partially oxidized interface of fluid metallic veins during the first stages of the thermal heating cycle [3]. The strain localization at different conditions suggests that the outer ligament of the laminas can easily break, so that the pressurized pore can be released, even at low temperatures, potentially giving rise to outgassing phenomena in coated part subjected to moderate temperatures. The presence of initial discontinuities such as laminas or set of subsurface defects in a subsurface layer is thus potentially more detrimental than single pores. Lumley [17] clearly illustrated the progression of small laminar defects into a single subsurface discontinuity causing the development of a blister. Accurate study of the HPDC filling process as related to die geometry and technological parameters can help to avoid critical conditions of laminas formation in regions where the development of blisters during heat treatment cycles can be expected for the specific HPDC components. On the other hand the results of the present study suggest that an accu-rate study of the die filling and intensification stage can help to reduce the development of blisters.

The present investigation confirmed the beneficial effect of having a relatively thick pore-free layer, often reported in literature. Its development has been carefully investigated by Chen [18], showing the existence and formation conditions of two substantially pore-free layers. A eutecticrich and fine layer can solidify coming into contact to the die during the filling stage and is not significantly affected by the following pressurization stage. Another, often inner, alpha-rich layer is formed during the pressure intensification stage, when high pressure is applied to suppress pores. Deep inside the cast part, the bulk microstructure solidified after the intensification stage manifests the typical porous struc-ture, with a range of reference inner pressures. Possible discontinuities in the first layer are characterized by low reference pressure values, thus they have low risks to develop blisters, while those in the second pore-free layer, particularly when the first one is completely lacking or extremely thin, could easily led to blister development. The condition leading to low impingement and the formation of the fine eutectic-rich and stronger structure should thus be met in the portion of cast part where the development of blister could be critical.

The mechanisms of blister development from subsurface discontinuities is investigated in the present paper for a case of specific aluminum casting alloy and for a combination of thermal, loading and geometrical parameters. The considered parameters are inherent to conventional HPDC processes and can, in principle, be extended and adopted to different casting processes as well as to a wider group of materials.

7. Conclusions

The formation of a blister during a heat treatment cycle from a material portion containing an ellipsoidal pressurized pore is modeled for

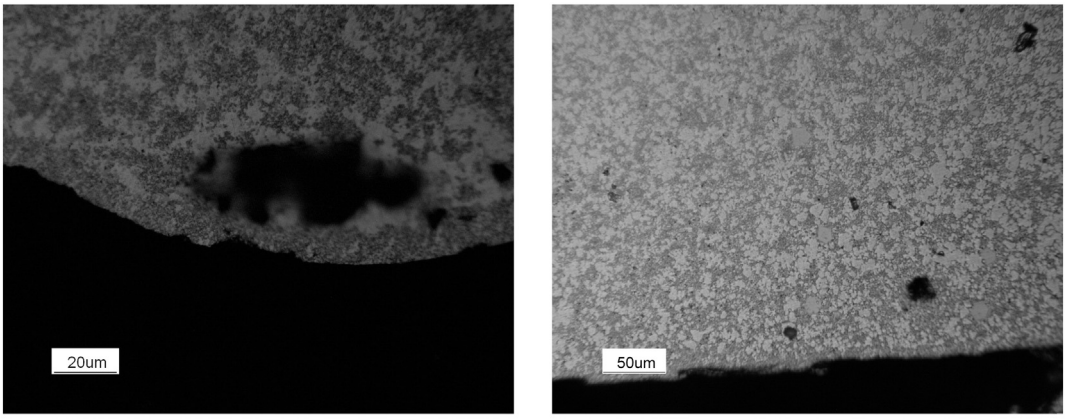

a) b)

Fig. 11. Metallographic sections of a HPDC part made of EN 46000 alloy heat treated at 350 °C showing subsurface pores with different *C*/*H* ratios and related to it: a) blister formation; b) the absence of blisters.

the case of an EN 46000 Al–9Si–3Cu–Fe alloy taking into account temperature-dependent elastoplastic behavior. FE simulations of the evolution of plastic strain fields and surface displacements during the thermal cycle for different defect shape, size, reference pressure and heat treatment suggest that several critical parameters for the blister formation can be identified. For a given defect shape (characterized by a fixed ratio of the ellipsoidal pore diameters) and relatively high inner pore pressures, a critical temperature for the development of blisters can be roughly estimated. At low inner pressure the identification of a critical temperature cannot be done easily due to the concurrent effect of many parameters defining the initial condition of the pore.

In addition to the conclusion to adopt process innovative HPDC reducing the pressure acting on the liquid, some useful suggestions can be derived to improve the resistance to blister formation of critical surfaces of conventional HPDC parts later to be subjected to thermal cycle. The most critical defects for blister formation are laminar discontinuities, and their formation should be carefully avoided in cast components to be later heat treated. Further, the analysis of the numerical results and of experimental validation tests suggested that attention should be paid to the development of a pore-free surface layer of sufficient thickness. The investigation can be potentially extended to different casting processes and materials where pressurized subsurface defects can be modeled similarly to those presented in this paper.

Acknowledgments

The authors are very grateful to GulioTimelli and Franco Bonollo (Department of Management and Engineering, University of Padova, Italy) for the supplied specimens for high-temperature tests and valuable discussions.

References

[1] E. Sjölander, Heat Treatment of Al–Si–Cu–Mg Casting AlloysPhD thesis Jönköping University, 2011.
[2] Lumley R, Odonnell R, Gunasegaram D, Givord, M. Heat treatment of high-pressure die castings. Metall. Mater. Trans. A2007;38A; 2564–74.
[3] E. Gariboldi, F. Bonollo, P. Parona, Handbook of Defects in High Pressure Diecastings, Associazione Italiana di Metallurgia, Milano, 2011.
[4] X. Niu, B. Hu, I. Pinwill, H. Li, Vacuum assisted high pressure die casting of alumini-um alloys, J. Mater. Process. Technol. 105 (2000) 119–127.
[5] P. Homayonifar, R. Babaei, E. Attar, S. Shahinfar, P. Davami, Numerical modeling splashing and air entrapment in high-pressure die casting, Int. J. Adv. Manuf. Technol. 39 (2008) 219–228.
[6] M. Thirugnanam, Modern high pressure die-casting processes for aluminium cast-ings, Trans. of 61st Indian Foundry Congress 2013, pp. 1–7.
[7] M. Uchida, Development of vacuum die-casting process, China foundry 6 (2009) 137–144.
[8] C. Garcia-Cordovilla, E. Louis, A. Pamies, The surface tension of liquid pure alumini-um and aluminium–magnesium alloy, J. Mater. Sci. 21 (1986) 2787–2792.
[9] M. Dargusch, G. Dour, N. Schauer, C. Dinnis, G. Savage, The influence of pressure dur-ing solidification of high pressure die cast aluminium telecommunications compo-nents, J. Mater. Process. Technol. 180 (2006) 37–43.
[10] H. Toda, P.C. Qu, S. Ito, K. Shimizu, K. Uesugi, A. Takeuchi, Y. Suzuki, M. Kobayashi, Formation behaviour of blister in cast aluminium alloy, Int. J. Cast Met. Res. 27 (2014) 369–377.
[11] J.E. Hatch, Aluminium: Properties and Physical Metallurgy, ASM International, Materials Park Ohio, 2004.
[12] G. Timelli, F. Bonollo, Quality mapping of aluminum alloy die castings, Metall. Sci. Technol. 26 (2008) 2–8.
[13] G. Timelli, S. Ferraro, F. Grosselle, F. Bonollo, F. Voltazza, L. Capra, Mechanical and microstructural characterization of diecast aluminium alloys, Metall. Ital. 103 (2011) 5–17.
[14] H. Hollomon, Trans. AIME 162 (1945) 268.
[15] R. Kuester, K.-H. Bode, W. Fritz, Beitrag zur Messung der Wärmeletfähigkeit von Metallen im Bereich von 0 bis 500 °C, Waerme- Stoffuebertrag. 1 (1968) 129–139 (in German).
[16] R.M. Jones, Deformation Theory of Plasticity, Bull Ridge Publishing, Blacksburg Virginia, 2009.
[17] R.N. Lumley, Progress on the heat treatment of high pressure diecastings, Fundamentals of Aluminium Metallurgy, Woodhead Publishing 2010, pp. 262–302.
[18] Z.W. Chen, Skin solidification during high pressure die casting of Al–11Si–2Cu–1Fe alloy, Mater. Sci. Eng. A348 (2003) 145–153.